

## ORIGINAL ARTICLE

# MiR-577 suppresses epithelial-mesenchymal transition and metastasis of breast cancer by targeting Rab25

Chonggao Yin<sup>1,2</sup>, Qingjie Mou<sup>3</sup>, Xinting Pan<sup>4</sup>, Guoxin Zhang<sup>3</sup>, Hongli Li<sup>3</sup> & Yunbo Sun<sup>4</sup> 

1 College of Nursing, Qingdao University, Qingdao, China

2 College of Nursing, Weifang Medical University, Weifang, China

3 Medicine Research Center, Weifang Medical University, Weifang, China

4 Intensive Care Unit, Affiliated Hospital of Qingdao University, Qingdao, China

**Keywords**Breast cancer; epithelial-mesenchymal transition; *MiR-577*; Rab25.**Correspondence**

Yunbo Sun, Intensive Care Unit, Affiliated Hospital of Qingdao University, No.16 Jiang Su Road, Qingdao, Shandong Province 266003, China.

Tel: +86 532 8261 1618

Fax: +86 532 8261 1618

Email: sunyunbo163@163.com

Received: 3 January 2018;

Accepted: 29 January 2018.

doi: 10.1111/1759-7714.12612

Thoracic Cancer 9 (2018) 472–479

**Abstract**

**Background:** MicroRNAs can act as both tumor suppressor genes and oncogenes and participate in cell proliferation, metastasis, and apoptosis. Low levels of *miR-577* are found in several cancers, for example, thyroid carcinoma, glioblastoma, and hepatocellular carcinoma. The aim of this study was to investigate the effect of *miR-577* on breast cancer (BC).

**Methods:** The relative level of *miR-577* in 120 BC tissues and cells was detected by real-time PCR. MDA-MB-231 cells with upregulated *miR-577* and MCF-7 cells with downregulated *miR-577* were established. Transwell invasion assays were used to examine the invasiveness of cells. Epithelial-mesenchymal transition (EMT) markers were evaluated by immunofluorescence and Western blot. Targeted combinations of *miR-577* and Rab25 were analyzed by luciferase assays. Xenograft models were used to examine the effect of *miR-577* on BC metastasis.

**Results:** *MiR-577* expression was significantly suppressed in BC tissues. Tumor size, tumor stage, and lymphatic metastasis were attributed to *miR-577* expression. Moreover, *miR-577* overexpression strongly inhibited the invasiveness and EMT of BC cells in vitro. *MiR-577* directly regulated Rab25 in BC. Rab25 upregulation by *miR-577* decreased the levels of E-cadherin and increased the levels of Vimentin. Notably, Rab25 knockdown inhibited BC invasion; however, an increase in Rab25 counteracted the invasive effect of *miR-577* in BC.

**Conclusion:** Results indicated that *miR-577* suppressed EMT by inhibiting Rab25 expression in BC. *MiR-577* and Rab25 are considered potential targets of BC treatment.

**Introduction**

Breast cancer (BC) is one of the most common malignant tumors in women. In 2014, approximately 14 million new cases and 8.2 million cancer deaths were recorded worldwide.<sup>1</sup> Before BC fully develops, it undergoes usual epithelial hyperplasia, atypical ductal hyperplasia, ductal carcinoma in situ, and invasive carcinoma.<sup>2</sup> Approximately 90% of patients with BC die of metastasis as a result of multiple steps and factors. Epithelial-mesenchymal transition (EMT) definitively causes invasion and distant migration of primary tumors.<sup>3</sup>

Epithelial-mesenchymal transition is a developmental process wherein epithelial cells lose their original properties and

acquire migratory traits of mesenchymal cells.<sup>4</sup> Moreover, EMT could promote invasion and metastasis. A crucial step in EMT is the downregulation of E-cadherin. Recent studies identified that microRNAs (miRNAs) are critical factors in EMT-related tumor metastasis.

MiRNAs are a series of small non-coding RNAs that could negatively regulate gene expression through complementarity to 3' -untranslated regions (UTRs) of messenger RNAs (mRNAs).<sup>5–7</sup> Recent studies have proven that miRNAs participate in biological processes, including cell proliferation, apoptosis, and metastasis.<sup>8</sup> Moreover, studies have discovered the multifaceted function of miRNAs in BC metastasis. MiR-200c inhibits metastasis of BC tumors

through the downregulation of Foxf2.<sup>9</sup> MiR-335 suppresses the migration and invasion of BC cells by targeting EphA4.<sup>10</sup> MiR-452 inhibits the migration and invasion of BC cells by directly targeting RAB11A.<sup>11</sup> MiR-140-5p inhibits angiogenesis and invasion by targeting VEGF-A in BC.<sup>12</sup> Hence, miRNAs and target genes could comprise an intricate network and play critical roles in BC metastasis.

Recent reports have demonstrated that *miR-577* deregulation is related to carcinogenesis. *MiR-577* could inhibit tumorigenesis of hepatocellular carcinoma via  $\beta$ -catenin.<sup>13</sup> Moreover, *miR-577* inhibits glioblastoma growth through the Wnt signaling pathway.<sup>14</sup> However, the functions of *miR-577* in BC remain unclear.

In this study, we elucidated the downregulation of *miR-577* in BC specimens and cells. However, the upregulation of *miR-577* reduced cell invasiveness. *MiR-577* downregulation also inhibited E-cadherin expression in BC cells by regulating Rab25. We conducted this study to facilitate the development of effective therapies for BC.

## Methods

### Patients and tissues

We obtained BC tissues (T) and adjacent non-tumor (ANT) tissues from patients at the Affiliated Hospital of Qingdao University from 2015 to 2016. All specimens were collected and frozen at  $-80^{\circ}\text{C}$ . None of the patients had received radiotherapy or chemotherapy before surgery. Informed consent was obtained from each patient. The Research Ethics Committee of Weifang Medical University approved the study.

### Cell culture

MCF-10A, MCF-7, MDA-MB-231 (MDA231), T47D, and MDA-MB-453 were obtained from American Type Culture Collection (Rockville, MD, USA). MCF-10A cells were cultured in Dulbecco's modified Eagle medium (DMEM)/F12, which contained 10% fetal bovine serum (FBS), 20 ng/mL epidermal growth factor, 0.1 mg/mL cholera toxin, 10 mg/mL insulin, and 500 ng/mL hydrocortisone. MCF-7 cells were cultured in minimum Eagle's medium containing 10% FBS and 1% sodium pyruvate. T47D, MDA-MB-453, and MDA231 cells were respectively cultured in RPMI1640 and DMEM containing 10% FBS, at  $37^{\circ}\text{C}$  in an atmosphere of 5%  $\text{CO}_2$ .

### Real-time PCR

Stem-loop quantitative (q)PCR was performed to determine the relative level of *miR-577*. U6 levels were used for normalization. We used TRIzol to extract RNA from fresh

BC tissues and cells. We synthesized complementary DNA with the total RNA using a M-MLV Reverse Transcriptase Kit (Promega, Madison, WI, USA). qPCR was carried out using an Applied Biosystems 7500 Real-time PCR System (Foster City, CA, USA). The following RT sequences were used: (5'-GTCGTATCCAGTGCAGGGTCCGAGGTATTCGACTGGATACGACCAGGTA-3'), forward primer (5'-ACCGCGCGCGCTAGATAAAAATATTGG-3'), and reverse primer (5'-ATCCAGTGCAGGGTCCGAGG-3').

### Cell transfection

*MiR-577* and negative control (NC) mimics, *miR-577* inhibitor NC, *miR-577* inhibitor, and small interfering RNAs (siRNAs), including Rab25 siRNA, were synthesized by GeneChem (Shanghai, China). We used Lipofectamine 2000 (Thermo Fisher Scientific, Waltham, MA, USA) to transfect the cells following the manufacturer's protocol. Rab25 complementary DNA was confirmed by DNA sequencing and was cloned into pcDNA3.1.

### Cell proliferation assays

For cell counting kit 8 (CCK-8; Solarbio, Beijing, China) assays, approximately  $2 \times 10^3$  cells were seeded in 96-well plates. After culture for 24, 48, 72, 96, and 120 hours, cell proliferation capacity was tested by CCK-8 assay. Cell growth curves were plotted using the absorbance value at each time point.

### Cell invasion assay

The invasion assay was assessed using Transwell chambers with Matrigel. After transfection, the cells were added to the upper chamber and incubated at  $37^{\circ}\text{C}$  for 24 hours. A total of 450  $\mu\text{L}$  of complete medium (RPMI 1640, 0.1% bovine serum albumin, and 25 mM 4-[2-hydroxyethyl]-1-piperazineethanesulfonic acid) with 3% FBS was placed in the bottom well. Cells that invaded through the membrane were fixed, stained, photographed, and counted overnight. All assays were repeated in triplicate.

### Immunofluorescence

A total of  $1 \times 10^4$  cells were planted in 24-well plates on slides overnight and cultured in serum-free medium for 12 hours. Cells were fixed using 4% paraformaldehyde for 25 minutes. Subsequently, the cells were permeabilized with 0.1% Triton X-100 and blocked with 5% bovine serum albumin for 30 minutes at  $37^{\circ}\text{C}$ . The cells were primarily incubated for 12 hours at  $4^{\circ}\text{C}$ . On the next day, cells were washed with phosphate buffered saline and incubated with Alexa Fluor 594 or Alexa Fluor 488-conjugated

secondary antibodies for 1 hour at 37°C. The nucleus was stained with 4',6-diamidino-2-phenylindole for 15 minutes. Finally, the pictures were collected and analyzed using a fluorescence microscope.

**Luciferase assays**

Cells ( $3.5 \times 10^4$ ) were planted in 24-well plates in triplicate overnight. A total of 100 ng mutant (MUT) or wild-type (WT) pGL3-Rab25-3'UTR and 1 ng of pRL-TK *Renilla* plasmid were transiently transfected according to the manufacturer's protocol. *Renilla* and luciferase signals were measured using the Dual-Luciferase Reporter Assay Kit (Promega).

**Western blot**

We used Western blot to analyze protein expression. Cell or tissue protein lysates were electrophoresed on 10% sodium dodecyl sulfate-polyacrylamide gel electrophoresis and transferred onto polyvinylidene fluoride membranes. We incubated the membranes with the following primary antibodies, obtained from Cell Signaling Technology (Danvers, MA, USA): Rab25, E-cadherin, Vimentin, and

$\beta$ -actin. We then incubated the membranes with horseradish peroxidase-linked anti-rabbit immunoglobulin G and anti-mouse immunoglobulin G antibodies (Cell Signaling Technology). All assays were repeated in triplicate.

**Statistical analysis**

We analyzed all statistical data using SPSS version 19.0 (IBM Corp., Armonk, NY, USA). A chi-square test was used to analyze the relevance between *miR-577* and Rab25 expression and clinicopathological features. A Student's paired two-tailed *t*-test or analysis of variance was used to analyze statistical significance.  $P < 0.05$  was considered significant in all cases.

**Results**

***miR-577* expression was decreased in breast cancer (BC) tissues and cells and is related to clinicopathological features**

We hypothesized the potential significance of *miR-577* in BC development and progression. We first detected

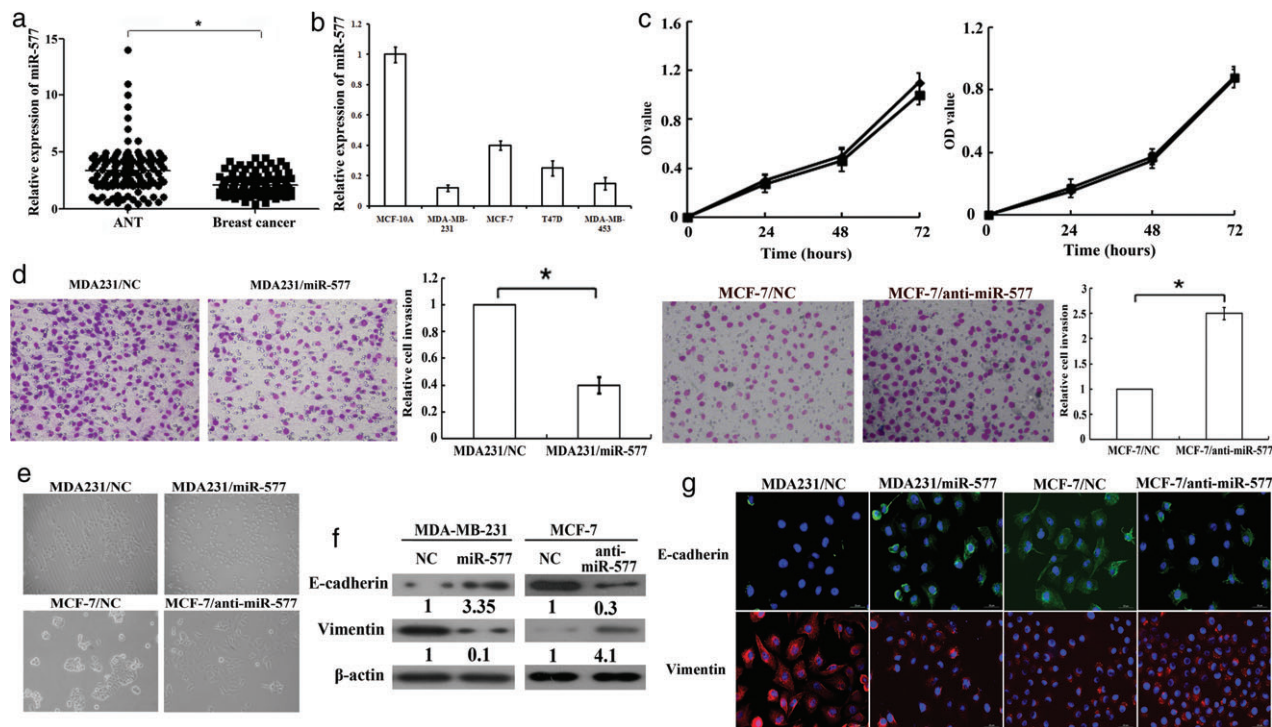


**Figure 1** Expression of *miR-577* was decreased in breast cancer (BC) tissues and cells and inhibited migration and invasion of BC cell lines in vitro. (a) Relative expression of *miR-577* in BC and adjacent non-tumor (ANT) tissues and (b) various BC cells. (c) Cell proliferation in MDA231 and MCF-7 was evaluated using cell counting kit 8 assay (—●—) MDA231/NC, (—■—) MDA231/miR-577, and (—◆—) MCF-7/NC, (—□—) MCF-7/anti-miR-577. (d) Invasion ability of MDA231 was analyzed by Transwell assay (quantification of penetrating cells, left). Transwell invasion assay of MCF-7/anti-miR-577 and MCF-7/NC cells (quantification of penetrating cells, right). (e) Morphological changes of MDA231 and MCF-7 after transfection. (f) Expression changes in E-cadherin and Vimentin after transfection. (g) Immunofluorescence staining. \* $P < 0.05$ . OD, optical density.

**Table 1** Correlation between *miR-577* expression and clinical pathologic features in breast cancer patients

Characteristics	Number of cases	<i>miR-577</i> expression		<i>P</i>
		Low (≤median)	High (>median)	
Age (years)				0.273
< 55	58	26	32	
≥ 55	62	34	28	
Tumor size (cm)				0.039*
≤ 2	88	39	49	
> 2	32	21	11	
Tumor stage				0.028*
I+ II	62	25	37	
III+ IV	58	35	23	
Lymph node metastasis				0.002**
Positive	63	23	40	
Negative	57	37	20	
ER				0.357
Positive	65	31	34	
Negative	55	29	26	
PR				0.361
Positive	63	34	29	
Negative	57	26	31	
HER-2				0.097
Positive	50	21	29	
Negative	70	39	31	
Ki67				0.030*
Positive	47	18	29	
Negative	73	42	31	

\*Significant difference ( $P < 0.05$ ); \*\*significant difference ( $P < 0.01$ ). ER, estrogen receptor; PR, progesterone receptor.

*miR-577* expression in 120 pairs of human BC and ANT tissues. *MiR-577* was suppressed almost twofold in BC compared to ANT tissues (Fig 1a). The relationship between *miR-577* and the clinicopathological characteristics of the BC patients is summarized in Table 1. Correlations between *miR-577* and age and the expression levels of estrogen receptor, progesterone receptor, and Her2 were not statistically significant. However, the results showed that *miR-577* was closely related to tumor size, tumor stage, Ki67 expression, and lymph node metastasis.

*MiR-577* expression in BC cells was considerably reduced compared to MCF-10A (Fig 1b). MCF-7 cells showed the highest expression of *miR-577*, and MDA231 cells the lowest. All results indicated that reduction of *miR-577* expression in BC cells and tissues may cause metastasis.

### ***MiR-577* inhibited the invasion of BC cells**

To determine the function of *miR-577* in BC progression, MDA231 cells were stably transfected with *miR-577* mimics or NC and MCF-7 were transfected with *miR-577* inhibitor (anti-*miR-577*) or NC. The proliferation rates in

cells with upregulation and downregulation of *miR-577* were unchanged (Fig 1c). We assessed the effect of *miR-577* on the invasiveness of MDA231 and MCF-7. *MiR-577* upregulation could remarkably decrease the invasiveness of MDA231 compared to NC (Fig 1d left). *MiR-577* downregulation in MCF-7 significantly increased its invasiveness (Fig 1d right). These results suggest that *miR-577* inhibits the invasion of BC cells.

### ***MiR-577* reversed epithelial-mesenchymal transition (EMT) of BC cells**

To investigate whether *miR-577* overexpression prevented BC cell invasion by inhibiting EMT, we observed the morphological changes in BC cells. MDA231/*miR-577* could induce significant morphological changes, transforming from a spindle to a cobblestone shape. MCF-7/anti-*miR-577* showed a contrary effect (Fig 1e). Western blot analysis was used to detect E-cadherin and Vimentin in all cells. E-cadherin expression was increased in MDA231, while Vimentin expression decreased in MDA231/*miR-577* cells compared to MDA231/NC cells (Fig 1f, left). In MCF-7/anti-*miR-577* cells, the expression of E-cadherin was downregulated and Vimentin upregulated (Fig 1f, right). The same results were observed after immunofluorescence staining (Fig 1g). As a result, *miR-577* repressed the EMT phenotype in BC.

### ***MiR-577* directly regulated Rab25**

We excavated target genes using TargetScan bioinformatics prediction software (Whitehead Institute for Biological Research, Cambridge, UK), and the results proved that Rab25 is a target gene of *miR-577* (Fig 2a). In addition, we tested the expression levels of Rab25 in MDA231/*miR-577* and MDA231/NC cells. Our results showed that the protein level of Rab25 significantly decreased with transient *miR-577* expression (Fig 2b), suggesting the important function of Rab25 in *miR-577*-induced cells. Rab25 expression in MCF-7/anti-*miR-577* and MCF-7/NC cells was simultaneously tested, and the protein level of Rab25 significantly increased with transient *miR-577* downregulation. Rab25 mRNA levels also significantly increased with transient *miR-577* downregulation (Fig 2c). To prove if the predictive binding site of *miR-577* on the 3'-UTR of Rab25 was responsible for this regulation, we cloned the WT or MUT Rab25 3'-UTR downstream of a luciferase reporter gene. Moreover, we co-transfected WT or MUT Rab25 vector and *miR-577* or anti-NC into 293T cells. The co-transfection of WT Rab25 3'-UTR and *miR-577* vector into 293T cells markedly reduced luciferase activity compared to NC and *miR-577*. The inverse results were observed in 293T cells, which were co-transfected with anti-*miR-577* and WT Rab25 3'-UTR (Fig 2d), suggesting that *miR-577*

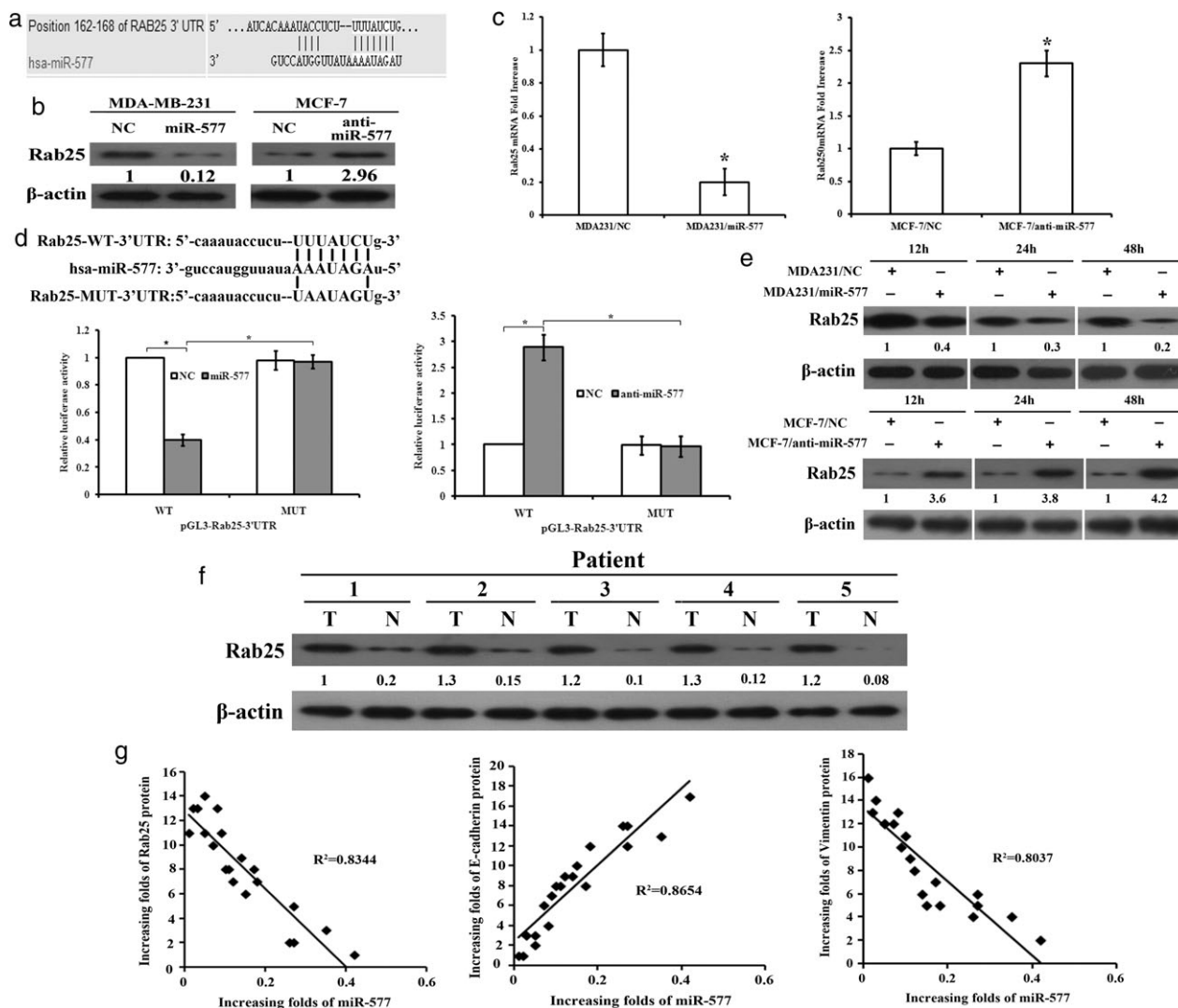


**Figure 2** *MiR-577* directly regulated Rab25. (a) Predictive binding of *miR-577* to the 3' untranslated region (UTR) of Rab25. (b) Rab25 and (c) Rab25 messenger RNA (mRNA) expression in MDA231 and MCF-7 after transfection. (d) Relative luciferase activity was detected in 293T cells after co-transfection with pGL3-WT or MUT Rab25 3' UTR and negative control (NC), *miR-577*, or anti-*miR-577*. Rab25 expression in (e) MDA231/NC and MDA231/*miR-577* cells, and MCF-7/NC and MCF-7/anti-*miR-577* cells; and (f) 10 paired BC and adjacent non-tumor (ANT) tissues. (g) Increasing folds of *miR-577* and Rab25, E-cadherin, and Vimentin in breast cancer relative to ANT tissues in each patient were counted. \**P* < 0.05. MUT, mutant; WT, wild type.

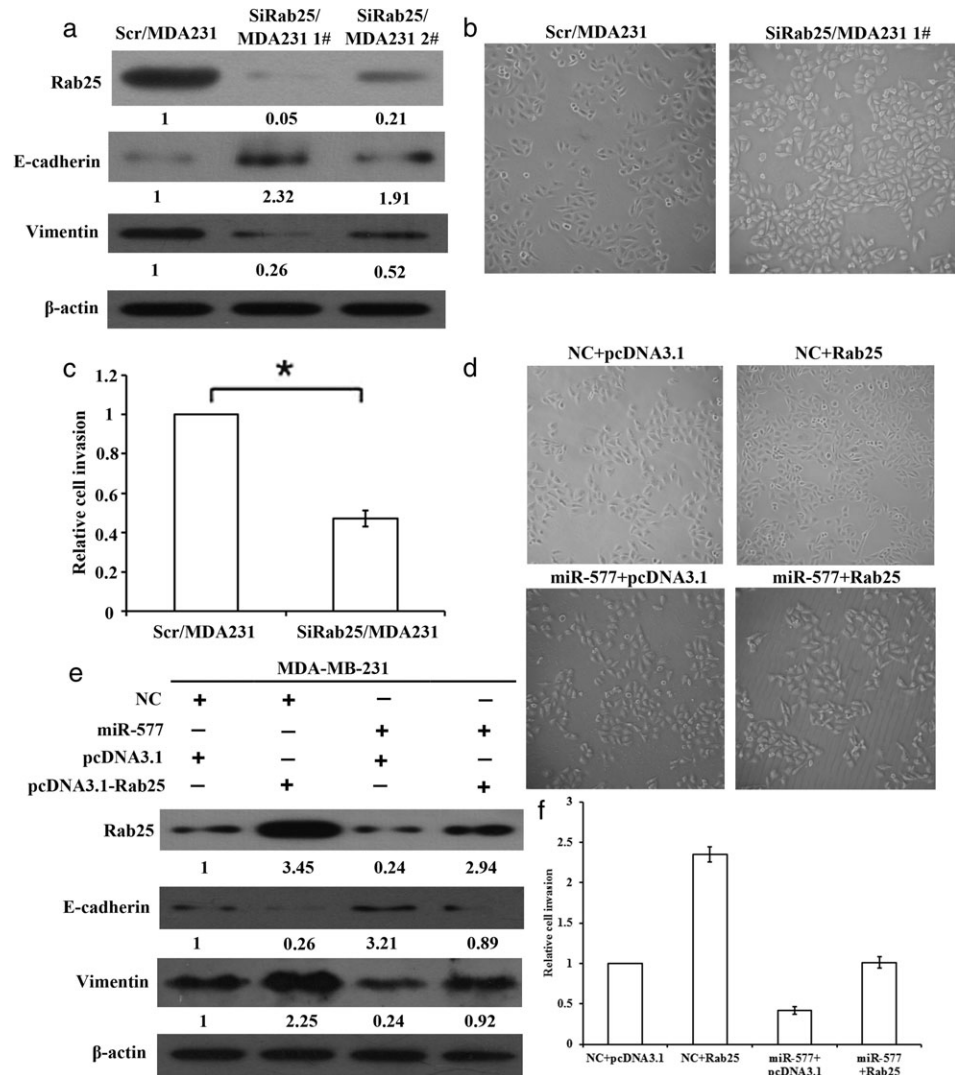
directly targets the 3'-UTR of Rab25 mRNA. The results indicate that *miR-577* downregulates Rab25 expression by binding its 3'-UTR.

To further confirm that *miR-577* directly binds with Rab25, *miR-577* and NC were transfected in at least 12 hours. Rab25 was decreased in MDA231/*miR-577* compared to MDA231/NC and reached the minimum level at 48 hours (Fig 2e). A similar result was observed in MCF-7 cells (Fig 2e). Moreover, an inverse correlation was observed among the expression levels of *miR-577* and Rab25, E-cadherin, and Vimentin in 10 tested clinical specimens (Fig 2f,g). These findings confirm that *miR-577* directly regulates Rab25.

### Rab25 participated in EMT-related invasion via *miR-577*

To explore whether Rab25 influences EMT-related invasion via *miR-577*, we transfected RNA interference Rab25 gene in MDA231 cells. Western blot detected Rab25 expression and resembled the EMT markers, and E-cadherin levels were increased with highly efficient knock-down, whereas Vimentin protein levels were decreased to a certain extent (Fig 3a). In particular, Rab25 suppression induced cell morphology, from a spindle to a cobblestone shape (Fig 3b), consistent with the effect of *miR-577*. The invasiveness of MDA231 cells transfected with siRNA

**Figure 3** Rab25 participated in epithelial-mesenchymal transition (EMT)-related invasion in breast cancer cells via *miR-577*. (a) Changes in E-cadherin and Vimentin levels, (b) morphological changes, and (c) relative cell invasion of MDA231 after transfection with small interfering Rab25 (siRab25) and control group transfection with scrambled-siRNA (Scr). (d) Morphological changes of MDA231. (e) Expression of Rab25 and EMT-related markers transfected with different plasmid. (f) MDA231 invasion using Transwell assay. \* $P < 0.05$ .



fragments was assessed using Transwell assay. The results indicated that Rab25 knockdown significantly impaired cell motility (Fig 3c). We transfected Rab25 and *miR-577* in MDA231 cells to determine whether Rab25 would offset the suppressing effect of *miR-577*. MDA231 cells were co-transfected with NC or *miR-577* and pcDNA3.1 or pcDNA3.1-Rab25. Rab25 overexpression can reciprocally neutralize, as shown by the morphological changes (Fig 3d). Vimentin was positively regulated, whereas E-cadherin was negatively regulated, along with the restoration of Rab25, as shown by Western blot analysis (Fig 3e). Transwell assays were performed to investigate the invasion of MDA231 cells. Reduction in the invasiveness initiated by *miR-577* in MDA231 cells was counteracted by Rab25 expression (Fig 3f). The results suggest that Rab25 is a functional target gene of *miR-577*.

### ***miR-577* overexpression and Rab25 reduction inhibited lung colonization of BC cells in SCID mice**

To further investigate the effect of *miR-577* and Rab25 on tumor metastasis in vivo, we adopted SCID mice with BC tumor xenografts. MDA231/NC, MDA231/*miR-577*, Scr/MDA231, and SiRab25/MDA231 cells were subcutaneously injected into each mouse. After eight weeks, all mice were sacrificed to harvest their xenografts and lungs. The metastatic nodules were smaller in the lungs of SCID mice injected with SiRab25/MDA231 or MDA231/*miR-577* compared to Scr/MDA231 and MDA231/NC groups (Fig 4a,b). Rab25 expression in the xenograft was lower in SCID mice injected with MDA231/*miR-577* and siRab25/MDA231 cells compared to MDA231/NC and Scr/MDA231 (Fig 4c). We also detected *miR-577* expression in tumors in SCID mice injected with

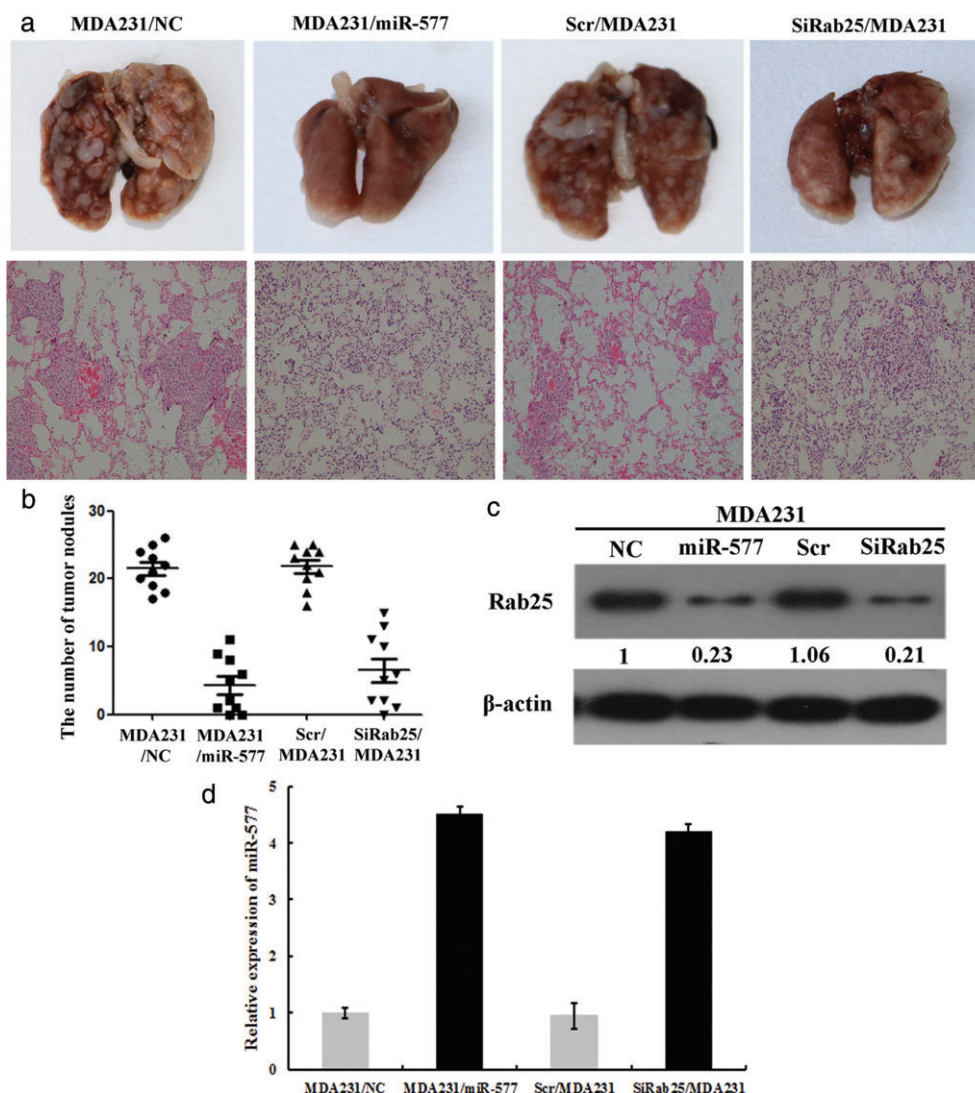


**Figure 4** *miR-577* overexpression and Rab25 reduction inhibited lung colonization of breast cancer (BC) cells in SCID mice. (a) Lung metastasis nodes in SCID mice implanted with MDA231/NC, MDA231/*miR-577*, scrambled-siRNA (Scr)/MDA231, and small interfering Rab25 (siRab25)/MDA231 cells visualized by hematoxylin and eosin staining. (b) The number of metastatic lung nodes was calculated. (c) Rab25 expression in MDA231 transfected with different plasmid. (d) *miR-577* expression was tested in SCID xenograft tumors. NC, negative control.

MDA231/NC, MDA231/*miR-577*, Scr/MDA231, and SiRab25/MDA231 cells. *miR-577* expression was remarkably increased in SCID mice injected with MDA231/*miR-577* and siRab25/MDA231 cells (Fig 4d). All of these results congruently indicate that *miR-577* inhibits lung colonization of BC cells in SCID mice.

## Discussion

Previous studies have shown that miRNAs can take effect as either oncogenes or tumor suppressor genes, resulting in oncogenesis and progression.<sup>15</sup> Moreover, one study suggested that *miR-577* is downregulated in colorectal cancer

specimens and cells. Restoration of *miR-577* significantly suppresses proliferation and induces a G0/G1 cell cycle arrest in colorectal cancer cells.<sup>16</sup> The relative expression of *miR-577* is lower in hepatocellular carcinoma tissues than in ANT. Low expression of *miR-577* is related to large tumor size and advanced tumor node metastasis stage.<sup>13</sup> Consistent with previous findings, we discovered that *miR-577* expression is markedly decreased in BC tissues compared to expression in paired ANT and *miR-577*, which serves as a tumor suppressor gene in BC.

Two primary factors in human cancers, especially for malignant tumors, are metastasis and invasion, of which EMT is a fundamental step. MicroRNA interprets an important role in the EMT of BC. MiR-520c-3p can

negatively regulate EMT by targeting IL-8 and suppresses the invasion and migration of BC.<sup>17</sup> MiR-381 inhibits proliferation, EMT, and metastasis of BC cells by targeting CXCR4.<sup>18</sup> Our results prove that *miR-577* reverses EMT in BC cells.

Rab25 is frequently amplified in cancers and is implicated in solid tumors. Rab25 expression enhances the aggressiveness of a subset of BC cells.<sup>19</sup> Mitra *et al.* showed that Rab25 acts as an oncogene in luminal B BC and is associated with snail-driven EMT.<sup>20</sup> Our results show that Rab25 influences the EMT-related invasion of BC cells. MiRNAs could negatively target gene expression through complementarity to 3'-UTRs of mRNAs and *miR-577* downregulated Rab25 expression. In short, the overexpression of Rab25 abolished the inhibitory effect of miR-577 on the invasion of BC cancer.

In summary, our findings imply that *miR-577* downregulation might result in the increased expression of Rab25, which promotes invasion and metastasis in BC cells *in vitro*. We might reasonably conclude that *miR-577* inhibits Rab25 and both may be suitable as potential therapeutic targets of BC.

## Acknowledgments

This study was supported by the National Nature Science Foundation of China (81702932, 81641111 and 81402389) and the Natural Science Foundation of Shandong Province (ZR2015HL065).

## Disclosure

No authors report any conflict of interest.

## References

- McGuire S. World Cancer Report 2014. Geneva, Switzerland: World Health Organization, International Agency for Research on Cancer, WHO Press, 2015. *Adv Nutr* 2016; **7**: 418–9.
- Pinder SE, Ellis IO. The diagnosis and management of pre-invasive breast disease: Ductal carcinoma in situ (DCIS) and atypical ductal hyperplasia (ADH)--current definitions and classification. *Breast Cancer Res* 2003; **5**: 254–7.
- Guarino M. Epithelial-mesenchymal transition and tumour invasion. *Int J Biochem Cell Biol* 2007; **39**: 2153–60.
- Kalluri R, Weinberg RA. The basics of epithelial-mesenchymal transition. *J Clin Invest* 2009; **119**: 1420–8 (Published erratum appears in *J Clin Invest* 2010;120:1786).
- Ventura A, Jacks T. MicroRNAs and cancer: Short RNAs go a long way. *Cell* 2009; **136**: 586–91.
- Calin GA, Croce CM. MicroRNA-cancer connection: The beginning of a new tale. *Cancer Res* 2006; **66**: 7390–4.
- Sun L, Zhang B, Liu Y, Shi L, Li H, Lu S. MiR125a-5p acting as a novel Gab2 suppressor inhibits invasion of glioma. *Mol Carcinog* 2016; **55**: 40–51.
- Iorio MV, Croce CM. microRNA involvement in human cancer. *Carcinogenesis* 2012; **33**: 1126–33.
- Zhang T, Wan JG, Liu JB, Deng M. MiR-200c inhibits metastasis of breast tumor via the downregulation of Foxf2. *Genet Mol Res* 2017. <https://doi.org/10.4238/gmr16038971>
- Dong Y, Liu Y, Jiang A, Li R, Yin M, Wang Y. MicroRNA-335 suppresses the proliferation, migration, and invasion of breast cancer cells by targeting EphA4. *Mol Cell Biochem* 2018; **439**: 95–104.
- Li W, Li G, Fan Z, Liu T. Tumor-suppressive microRNA-452 inhibits migration and invasion of breast cancer cells by directly targeting RAB11A. *Oncol Lett* 2017; **14**: 2559–65.
- Lu Y, Qin T, Li J *et al.* MicroRNA-140-5p inhibits invasion and angiogenesis through targeting VEGF-A in breast cancer. *Cancer Gene Ther* 2017; **24**: 386–92.
- Wang LY, Li B, Jiang HH, Zhuang LW, Liu Y. Inhibition effect of *miR-577* on hepatocellular carcinoma cell growth via targeting beta-catenin. *Asian Pac J Trop Med* 2015; **8**: 923–9.
- Zhang W, Shen C, Li C *et al.* *miR-577* inhibits glioblastoma tumor growth via the Wnt signaling pathway. *Mol Carcinog* 2016; **55**: 575–85.
- Chen CZ. MicroRNAs as oncogenes and tumor suppressors. *N Engl J Med* 2005; **353**: 1768–71.
- Jiang H, Ju H, Zhang L, Lu H, Jie K. microRNA-577 suppresses tumor growth and enhances chemosensitivity in colorectal cancer. *J Biochem Mol Toxicol* 2017; **31** (6): e21888.
- Tang CP, Zhou HJ, Qin J, Luo Y, Zhang T. MicroRNA-520c-3p negatively regulates EMT by targeting IL-8 to suppress the invasion and migration of breast cancer. *Oncol Rep* 2017; **38**: 3144–52.
- Xue Y, Xu W, Zhao W, Wang W, Zhang D, Wu P. miR-381 inhibited breast cancer cells proliferation, epithelial-to-mesenchymal transition and metastasis by targeting CXCR4. *Biomed Pharmacother* 2017; **86**: 426–33.
- Cheng KW, Agarwal R, Mitra S *et al.* Rab25 increases cellular ATP and glycogen stores protecting cancer cells from bioenergetic stress. *EMBO Mol Med* 2012; **4**: 125–41.
- Mitra S, Federico L, Zhao W *et al.* Rab25 acts as an oncogene in luminal B breast cancer and is causally associated with Snail driven EMT. *Oncotarget* 2016; **7**: 40252–65.